JSHC
Japan Society of
Histochemistry and Cytochemistry
Established 1959

Acta Histochem. Cytochem. 57 (6): 199–209, 2024
doi: 10.1267/ahc.24-00049

*Regular Article*

# Alterations in Ileal Secretory Cells of The DSS-Induced Colitis Model Mice

**Kenta Nakamura[1,2], Ryoko Baba[2], Keiji Kokubu[2], Masaru Harada[1] and Hiroyuki Morimoto[2]**

*[1]Third Department of Internal Medicine, University of Occupational and Environmental Health, 1–1, Iseigaoka, Yahatanishi, Kitakyushu, Fukuoka 807–8555, Japan and [2]Department of Anatomy, School of Medicine, University of Occupational and Environmental Health, 1–1, Iseigaoka, Yahatanishi, Kitakyushu, Fukuoka 807–8555, Japan*

Received September 7, 2024; accepted October 18, 2024; published online December 17, 2024

Inflammatory bowel disease is triggered by abnormalities in epithelial barrier function and immunological responses, although its pathogenesis is poorly understood. The dextran sodium sulphate (DSS)-induced colitis model has been used to examine inflammation in the colon. Damage to mucosa primality occurs in the large intestine and scarcely in the small intestine. To evaluate the effect on the ileum, we histologically analyzed the inflammatory and recovery phases in DSS model mice, and 40 kDa FITC-dextran was used to investigate barrier function. In the inflammatory phase, histological damage was insignificant. However, expanded crypts, hypertrophic goblet and Paneth cells, increased mucus production and secretion were observed. The cellular morphology was restored to that of the control in the recovery phase. According to *in situ* hybridization and lectin histochemistry, the expression of intestinal stem cell markers, secretory cell differentiation factors, and glycosylation of secretory granules in Paneth cells differed in the DSS model. DSS-treatment did not influence the barrier function in the ileum, and FITC-dextran did not diffuse *via* the paracellular pathway into the mucosa. However, cells incorporating FITC appeared even under normal conditions. The number of FITC-positive Paneth cells was lower in the DSS group than the control group. Our results showed morphological and functional alterations in ileal epithelial cells, especially secretory cells, in the DSS colitis model.

**Key words:** ileum, DSS induced colitis, Paneth cell, goblet cell

## I. Introduction

The small intestine is essential for digestion and absorption through its mucosa. The mucous membranes contain numerous villi and crypts. Crypts are areas of cell proliferation at the base of villi. Epithelial cells actively proliferate and are renewed approximately every 5 days in the crypts. Intestinal stem cells (ISC) are *Lgr5*-positive crypt base columnar (CBC) cells located at the crypt base [3]. Cells located at the fourth position from the crypt base (+4 cells) are also considered ISC [28, 29]. These +4 cells work as backup ISCs when *Lgr5* cells are dysfunctional [1, 6, 24]. *Lgr5*-positive stem cells are self-renewing and multi-potent cells that differentiate into various small intestinal epithelial cells [4], including absorptive, goblet, Paneth, endocrine, tuft, and M cells.

Goblet cells secrete mucin, a glycoprotein that is the main component of mucus, to maintain homeostasis in the intestinal mucosa. The mucous layer prevents the invasion of bacteria into the epithelium, thereby playing a role in innate immunity. Goblet cells are also active regulators of the acquired immune system, accumulating antigens in the lumen through endocytosis and transmitting signals to specific dendritic cells [21, 22, 27]. Goblet cells have been reported to interact with the bacterial flora and immune system [40]. Many studies have investigated the relation-

Correspondence to: Ryoko Baba, Ph.D., Department of Anatomy, School of Medicine, University of Occupational and Environmental Health, 1–1, Iseigaoka, Yahatanishi, Kitakyushu, Fukuoka 807–8555, Japan.
E-mail: babar@med.uoeh-u.ac.jp

ship between bacterial infections, inflammation, and goblet cells [27]. Bacterial (*Vibrio parahaemolyticus* and *Vibrio cholerae*), viral, and parasitic infections can affect the goblet cell number and secretion of mucus into the small intestinal lumen [31, 32, 45]. Ulcerative colitis (UC) is an inflammatory bowel disease (IBD) characterized by a decrease in the number of goblet cells and mucus in the colon during the active phase [10]. A decrease in goblet cells is thought to a result from suppression of normal differentiation, leading to abnormal mucus secretion [26, 46]. In UC and Crohn's disease (CD), colonic goblet cells produce abnormal glycosylated mucin, which tends to acidify [23, 30, 33, 45].

Paneth cells are another type of secretory cells in the small intestinal crypts. They secrete antimicrobial peptides such as α-defensin and participate in host defense and maintain homeostasis through the intestinal flora [7]. Paneth cells also express epidermal growth factor (EGF), Wnt3, and the cell surface molecule Dll4, and play an important role in the establishment of a niche that maintains ISCs [34]. Paneth cells are found in the cecum and ascending colon of humans as well as in small intestinal crypts, but are uncommon in the descending colon and rectum. However, in patients with UC and CD, there was a significant increase in Paneth cells in the large intestine, excluding the cecum, compared to healthy controls [37]. Loss or reduction of Paneth cells has been reported in cases of ileal CD, ischemic enteritis, necrotizing enterocolitis, pathogenic bacterial enteritis, graft-versus-host disease (GVHD), and HIV-associated cryptosporidiosis [9, 18, 36]. Abnormal Paneth cell function (autophagy abnormalities, abnormal granule secretion, impaired pathogen-associated molecular patterns (PAMP) recognition, altered defensin production, or aberrant endoplasmic reticulum (ER) stress) has been reported to be associated with the onset of CD [36, 44].

Oral administration of dextran sodium sulphate (DSS) in drinking water is widely used to induce colitis in mice and rats [8, 41]. In DSS-induced colitis, severe symptoms (epithelial damage, crypt disappearance, and inflammation) are observed in the large intestine. Therefore, the usefulness of such mice and rats as models for research on large bowel inflammation has been evaluated. The small intestine of the DSS-colitis model is believed to be unaffected and has not been extensively investigated. It has been reported that DSS-colitis does not change the number of Paneth cells in the small intestine [30]. However, a close relationship between colitis and Paneth cells has been suggested by the metaplasia of Paneth cells observed in colonic inflammation, although the correlation between small intestinal Paneth cells and colitis during inflammation has not been explored.

A small number of UC patients have an inflammation of the terminal ileum, called backwash ileitis. The pathogenesis of the disease is not clearly understood. Ileitis occurred even in patients with ulcerative proctitis and left-sided UC [15, 43]. In these cases, the hypothesis of ileocecal valve dysfunction is not applicable and other pathogenic mechanisms that interact the small intestine and colitis, have been suggested.

In this study, we investigated how secretory cells of the small intestine, including goblet and Paneth cells, are affected by DSS-induced colitis.

## II. Materials and Methods

### *Animals*

In this study, 8-week-old male C57BL/6 J mice (CLEA Japan, Tokyo, Japan) were used. DSS (M.W. = 36,000–50,000; MP Biomedicals, Fountain Parkway Solon, OH, USA) was dissolved in autoclaved water to produce a 2% DSS solution. Mice were provided with the solution *ad libitum* for 7 days, and from day 8, they were allowed to drink autoclaved water (Fig. 1A). Mice were checked daily for body weight, fecal condition, and hematochezia. The inflammatory phase was evaluated on the 7th day of DSS administration, and the recovery phase was evaluated on the 14th day, compared to control mice. For the control, mice that were kept untreated for 14 days were used.

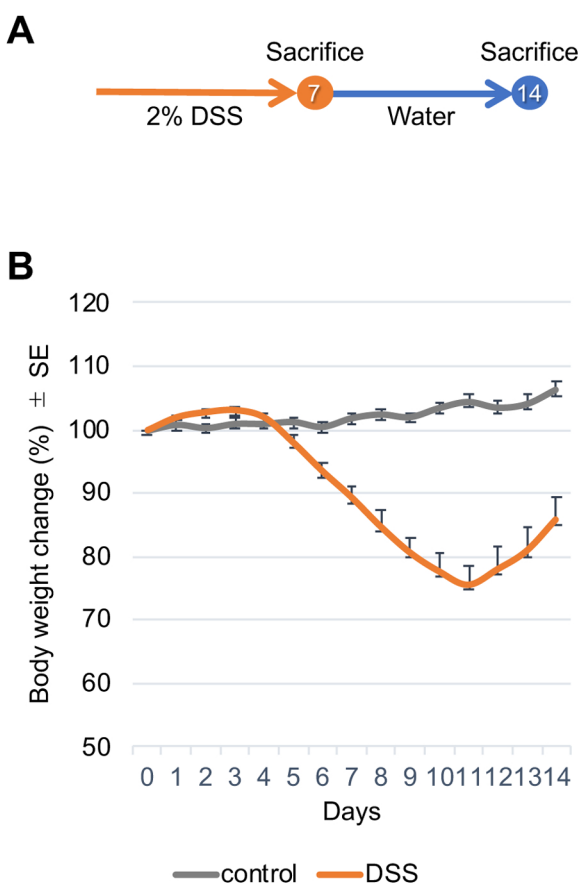


**Fig. 1.** **A**) Experimental design for the DSS colitis mouse model. Mice were euthanized on day 7 in the inflammation phase and on day 14 in the recovery phase. **B**) Percent mean ± standard error of the original body weight for 14 days.

For morphological analysis, mice were injected intraperitoneally with a mixture of anesthetics (medetomidine, midazolam, and butorphanol), the abdominal wall was longitudinally incised, and the ileum and distal colon were excised. To examine epithelial barrier function, mice were injected with FITC-dextran 40 kDa (Sigma-Aldrich, St. Louis, MO, USA) into the intestinal lumen for 1 hr under anesthesia. FITC-dextran was used at a concentration of 0.3 mg/g body weight in 200 μl of 0.1 M sodium phosphate buffer (PBS; pH 7.4). Other mice were injected with sodium fluorescein (FITC, FUJIFILM Wako Pure Chemicals, Osaka, Japan) alone or FITC in combination with dextran 40 kDa (FUJIFILM Wako Pure Chemicals). The research protocol was approved by the Ethics Committee of the University of Occupational and Environmental Health (Institutional Review Board approval number: AE20-009) and was conducted in accordance with the regulations of the 1995 Declaration of Helsinki (revised in Edinburgh in 2000).

***Hematoxylin and eosin staining***

The ileal and distal colon tissues were fixed with 4% paraformaldehyde in PBS at 4°C for 16 hr. The tissues were embedded in paraffin, and 5-μm sections were prepared. Samples were subjected to hematoxylin and eosin (H-E) staining according to standard methods [2]. Briefly, specimens were deparaffinized with xylene and alcohol, stained with hematoxylin for 15 min, and washed under running water for 15 min. After eosin staining for 7 min, the samples were dehydrated with ethanol and xylene and mounted.

***Immunohistochemistry***

The specimens were deparaffinized, immersed in 10 mM citrate buffer (pH 6.0), and antigen retrieval was performed for 15 min in a microwave (MI-33, Azumaya, Tokyo, Japan). Non-specific reactions were blocked with Blocking One Histo solution (Nacalai Tesque, Kyoto, Japan) for 10 min at 25°C. After washing with 0.1% tween20-PBS (PBS-T), the primary antibody (Table 1) was reacted at 4°C for 16 hr and the secondary antibody at 25°C for 1 hr. Tyramid signal amplification (Tyramid Super Boost Kit, Invitrogen, Thermo Fisher Scientific, Waltham, MA, USA) and microwave irradiation were performed for multiple immunostaining [38]. Briefly, the specimens were incubated with primary antibody for 1 hr at 25°C. After washing, the slides were incubated with horseradish peroxidase (HRP)-conjugated secondary antibody for 30 min, and tyramid amplification was performed. The samples were then immersed in citrate buffer and microwaved for 15 min to eliminate the primary antibody reactions. The antibody reaction was performed three times with different primary antibodies. The tyramid reagents used were Alexa Fluor 488, 555, and 647. Autofluorescence of the samples was suppressed using a Vector TrueVIEW Autofluorescence Quenching Kit (Vector Laboratories, Burlingame, CA, USA). Coverslips were mounted with a mounting medium containing 4',6-diamidino-2-phenylindole (DAPI). After mounting, the specimens were observed under a fluorescence microscope (Axio Imager M2, ApoTome.2, Carl Zeiss AG, Jena, Germany).

***In situ hybridization***

*In situ* hybridization was performed to detect gene expression [17]. We used the RNAscope system (Advanced Cell Diagnostics, Newark, CA, USA) according to the method provided in the manufacturer's instructions. The sections were hybridized with a specific c-RNA probe for mice, *Atoh1* (Mm-Atoh1, 40879) or *Lgr5* (Mm-Lgr5-01, 542031), and reacted with the alkaline phosphatase substrate Fast Red. We also immunohistochemically stained the same sections with anti-lysozyme and anti-OLFM4 antibodies and reacted them with the HRP substrate diaminobenzidine (DAB).

***Lectin histochemistry***

To analyze the glycosylation of secreted substances by secretory cells, deparaffinized sections were reacted with labeled lectin (Table 1) for 1 hr at 25°C [14]. After washing three times with PBS-T, coverslips were mounted with a mounting medium. After mounting, the specimens were observed under a fluorescence microscope (Axio Imager M2, ApoTome.2, Carl Zeiss AG, Jena, Germany). As a negative control experiment, we replaced lectins with PBS and performed the same reaction to confirm that there was no non-specific binding of lectins.

***Statistical analysis***

Data are expressed as the mean ± standard error. Differences between groups were evaluated using the Games-Howell test. Differences were considered statistically significant at a $p$-value of less than 0.05.

**Table 1.** *Antibodies and lectins*

| | | Bender | Dilution | RRID |
|---|---|---|---|---|
| OLFM4 | Rabbit monoclonal | Cell Signaling Technology (Danvers, MA, USA) | 1:200 | RRID:AB_2798465 |
| Mucin 2 (MUC2) | Rabbit polyclonal | Santa Cruz Biotechnology (Santa Cruz, CA, USA) | 1:200 | RRID:AB_2146667 |
| Lysozyme | Rabbit monoclonal | Abcam (Cambridge, UK) | 1:1000 | RRID:AB_10861277 |
| Wheat Germ Agglutinin (WGA) Alexa350 conjugate | Specifically recognizes N-acetylglucosamine | ThermoFisher Scientific (Waltham, MA, USA) | 1:300 | |
| Ulex Europaeus Agglutinin 1 (UEA 1) Rhodamine | Specifically recognizes α-1,2-fucose | Vector Laboratories (Burlingame, CA, USA) | 1:300 | |

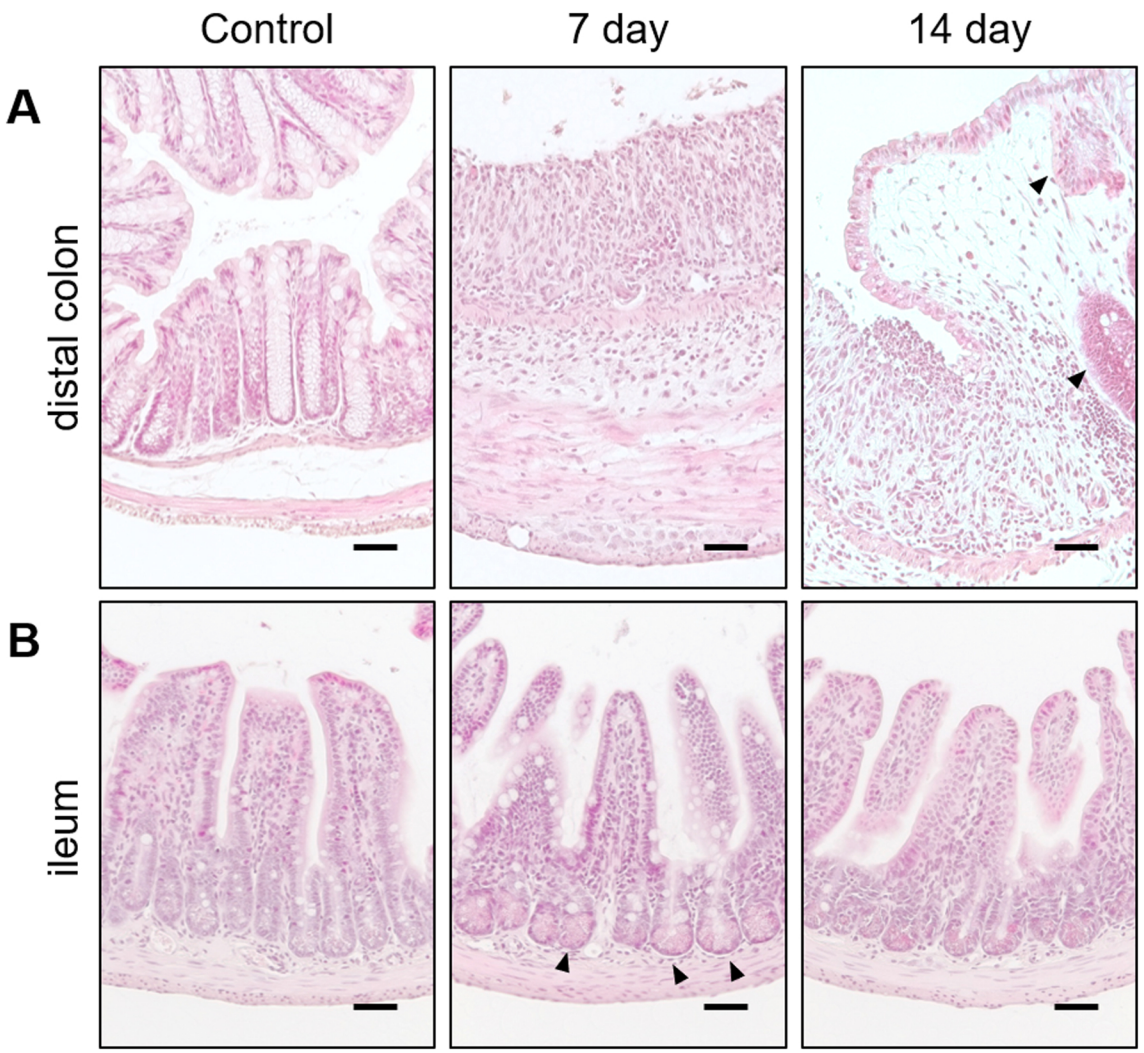


**Fig. 2.** **A**) Hematoxylin and eosin (H-E) staining of the distal colon from control and DSS mice on days 7 and 14. On day 7, crypts disappeared. The arrowhead indicates a crypt-like structure. **B**) H-E staining of the ileum from control and DSS mice on days 7 and 14. On day 7, crypts showed a round and expanding shape (arrowhead). Bars = 50 μm.

## III. Results

### *DSS-induced colitis model mice*

Mice administered DSS (n = 9) drank a 2% DSS solution at a rate of approximately 4.69 ml/mouse/day. The mice in the control group showed a slight increase in body weight during the experiment. In the DSS group, body weight decreased from the fifth day of the experiment and was approximately 75% of the initial body weight on the eleventh day. Subsequently, on the 12th day, the body weight began to increase and eventually recovered to 85% (Fig. 1B). Histological analysis showed that crypt structures in the mucosa were abolished, and muscular hypertrophy occurred in the distal colon on day 7. On day 14, the surface of the lumen was covered with columnar epithelial cells, and crypt-like structures (arrowheads) appeared. However, the distal colon of the day 14 did not recover to the morphology of the control (Fig. 2A).

Compared to the distal colon, there was no significant damage to the ileal structure, such as reduced villi or epithelial cell shedding, on days 7 and 14 (Fig. 2B). However, the crypts were enlarged in the ileum on day 7 compared to the control (Fig. 2B, arrowheads), and the crypt size of the ileum on day 14 was almost the same as that of the control. The enlarged crypts exhibited hypertrophic epithelial cells.

### *Changes in ileal epithelial cells of DSS-induced colitis*

To identify cell types affected by DSS, immunohistochemistry was performed using cell markers (Fig. 3). In the control, Muc2-positive epithelial cells were scattered throughout the villi and crypts, and lysozyme-positive cells were found at the bottom of the crypts (Fig. 3A). Moreover, stem cell marker (OLFM4)-positive cells were found as narrow cytoplasm between and above the cells with large cytoplasm (Fig. 3B). Secreted OLFM4 was also observed

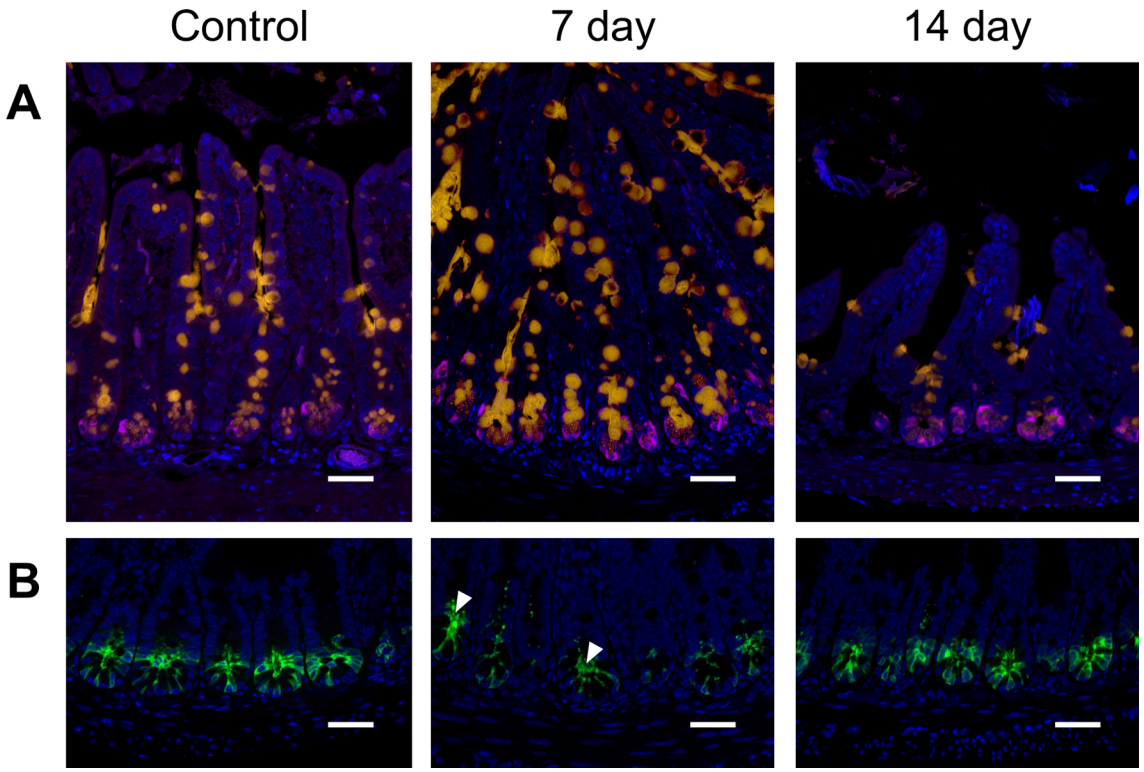


**Fig. 3.** **A**) Immunofluorescence analysis of the ileum from control and DSS mice on days 7 and 14. Merged images of the Paneth cell marker lysozyme (magenta), goblet cell marker Muc2 (orange), and nuclei (DAPI). **B**) Images of the intestinal stem cell marker OLFM4 (green) and nuclei (DAPI). Bars = 50 μm.

in the lumen of the crypts (Fig. 3B, arrowhead). On day 7, Muc2-positive secretions were observed in the lumen. Compared to the control, larger Muc2-positive structures were found in epithelial cells. Hypertrophic epithelial cells in the crypts were positive for lysozyme, and OLFM4-positive cells decreased, but their positions were the same as those in the control. On day 14, lysozyme- and OLFM4-positive cells had a similar morphology to those in the control, but Muc2-positive structures within epithelial cells were smaller than those in the control.

To investigate the state of cell differentiation in the ileal epithelium, *in situ* hybridization was performed (Fig. 4). Secretory cell differentiation factor (*Atoh1*)-positive cells were present in the crypts and villi in the control group. On day 7, the number of positive cells was low and the reaction was weak. However, on day 14, the number of positive cells increased and the reaction was enhanced (Fig. 4A). In the control, stem cell marker (*Lgr5*)-positive cells were located at the bottom of the crypt in the control, and on day 14 of the ileum. On day 7, few *Lgr5*-positive cells were observed between and above Paneth cells with characteristic granules. There were no coincidence *Lgr5*-positive cells and OLFM4-positive cells (Fig. 4B).

We also examined the effect of DSS-induced colitis on the glycosylation of secretory cell products (Fig. 5). Sections were reacted with lectins that recognize *N*-acetylglucosamine (WGA) and α-1,2-fucose (UEA 1). In the control, mucus granules in goblet cells reacted with WGA alone (line arrow) or with WGA and UEA 1 (arrow; Fig. 5 upper panels). In contrast, secretory granules of Paneth cells reacted with both WGA and UEA 1 (Fig. 5A, arrowhead and Fig. 5B). On day 7, the reaction of UEA 1 was weaker in Paneth cells; yet, the reaction in goblet cells was the same as that in the control. On day 14, the glycosylation of Paneth cells recovered to the same level as that of the control mice (Fig. 5B).

***FITC-dextran uptake by ileal epithelial cells in DSS-induced colitis***

To determine the protective barrier of the epithelium, FITC-dextran was administered to the intestinal tract. FITC-dextran did not penetrate the epithelium, both in the control and DSS-treated mice. However, some cells took up FITC-dextran, even under normal conditions. FITC-dextran–positive epithelial cells were dispersed in the villi and crypts. The distribution of FITC-positive cells in control mice varied among the crypts.

To identify the cell type of FITC-positive cells, specific cell markers were detected using immunohistochemistry. FITC-positive cells in the crypt base corresponded to OLFM4-positive cells with narrow cytoplasm (Fig. 6A, line arrow). Regarding secretary-type cells, Muc2 single-positive (arrow) cells in crypts and villi or lysozyme and Muc2 double-positive (arrowhead) cells at the base of

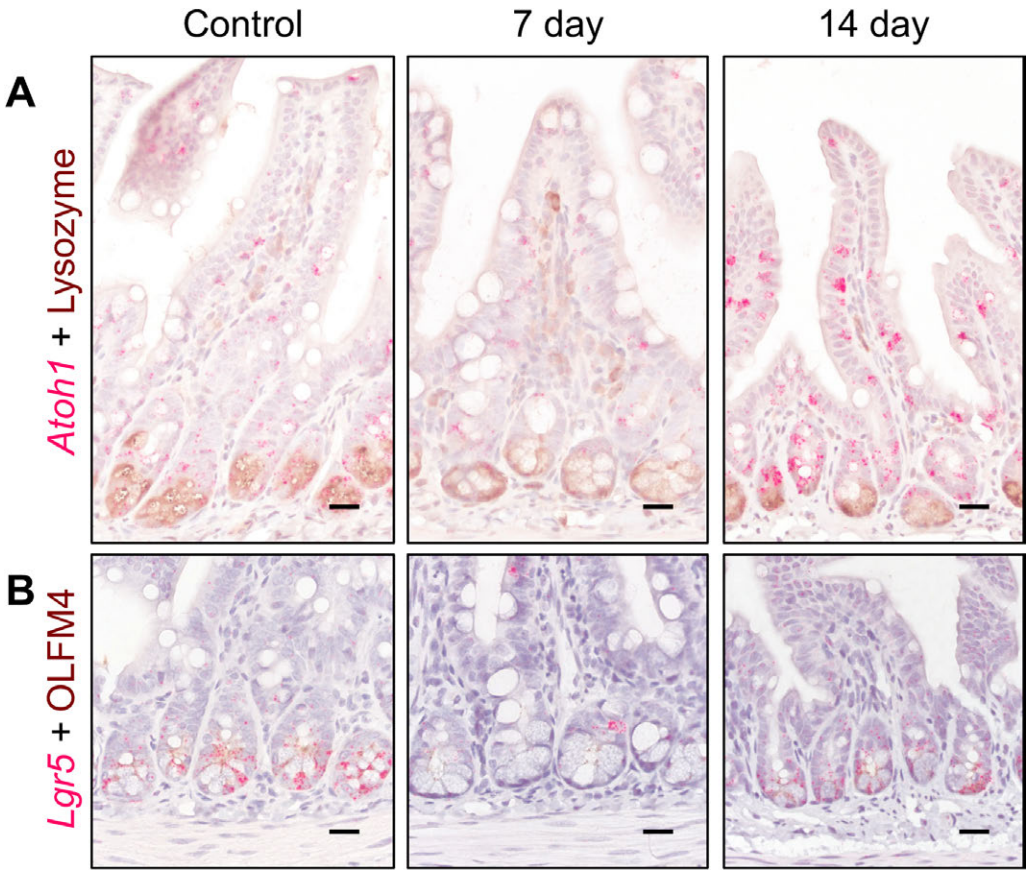


**Fig. 4.** **A**) *In situ* hybridization of *Atoh1* (red) and immunohistochemistry of lysozyme (brown) in the ileum. **B**) *In situ* hybridization of *Lgr5* (red) and immunohistochemistry of OLFM4 (brown) in the ileum. Bars = 20 µm.

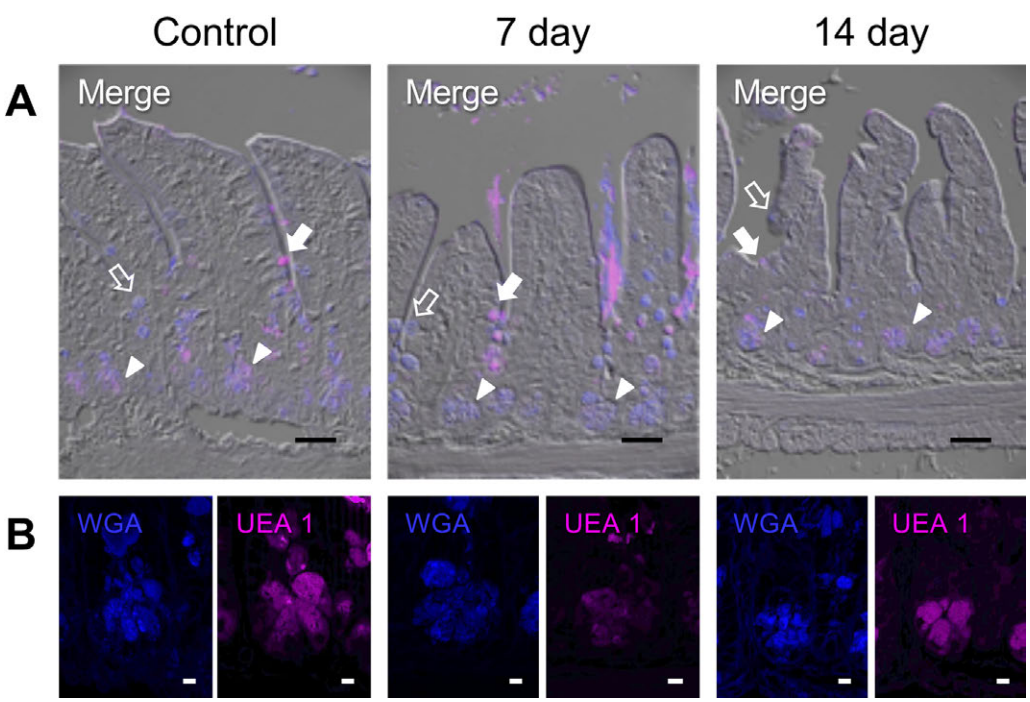


**Fig. 5.** **A**) Merged image of WGA-Alexa fluor 350 (blue), UEA 1-rhodamine (magenta), and phase-contrast image. Bars = 50 µm. **B**) High-magnification images of lectin histochemistry of WGA-Alexa 350 conjugate or UEA 1-rhodamine. Bars = 10 µm.

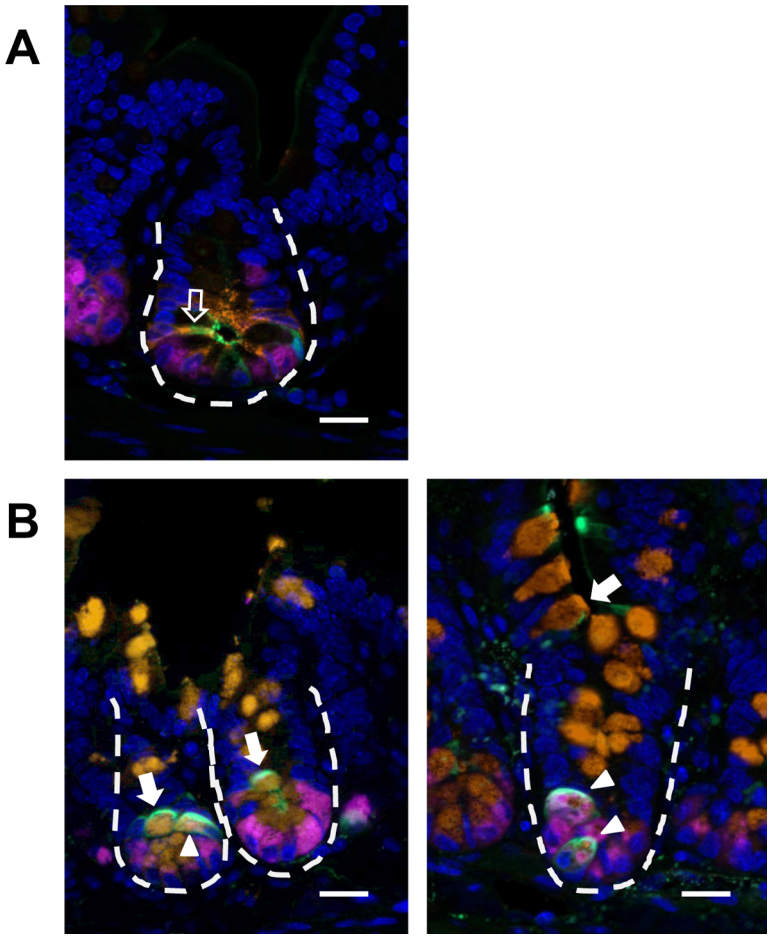


**Fig. 6.** Immunofluorescence analysis of the control ileum. FITC-dextran-positive cells were consistent with OLFM4 single-positive (line arrow), Muc2 single-positive (arrow), and lysozyme and Muc2 double-positive cells (arrowhead). **A**) FITC-dextran (green), lysozyme (magenta), OLFM4 (orange), and nuclei (DAPI). **B**) FITC-dextran (green), lysozyme (magenta), Muc2 (orange), and nuclei (DAPI). Crypts are outlined with a dashed line. Bars = 20 μm.

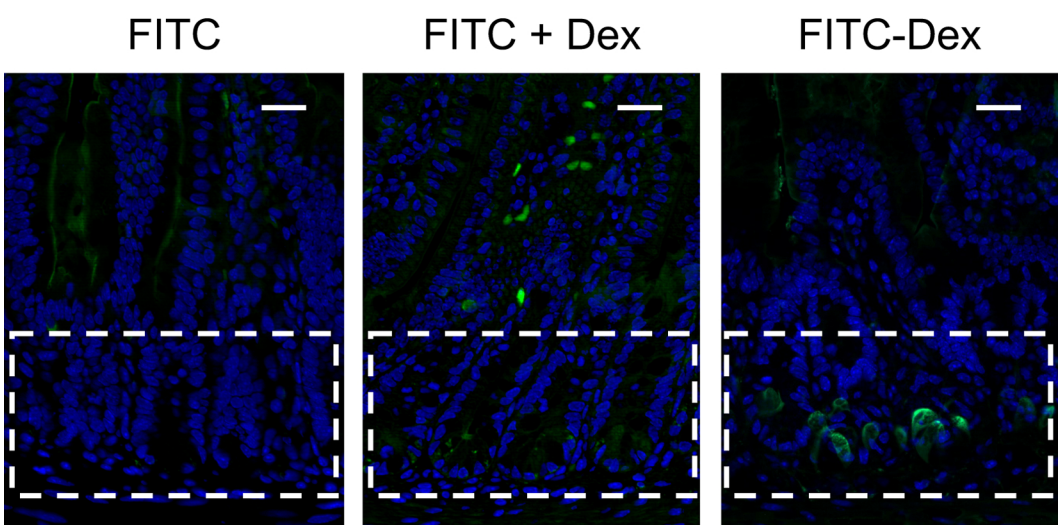


**Fig. 7.** Uptake of FITC, FITC in combination with dextran (FITC + Dex), or FITC-dextran (FITC-Dex) in the ileum. FITC and FITC-dextran are in green and nuclei are in blue (DAPI). The dashed square shows the crypt zone. Bars = 50 μm.

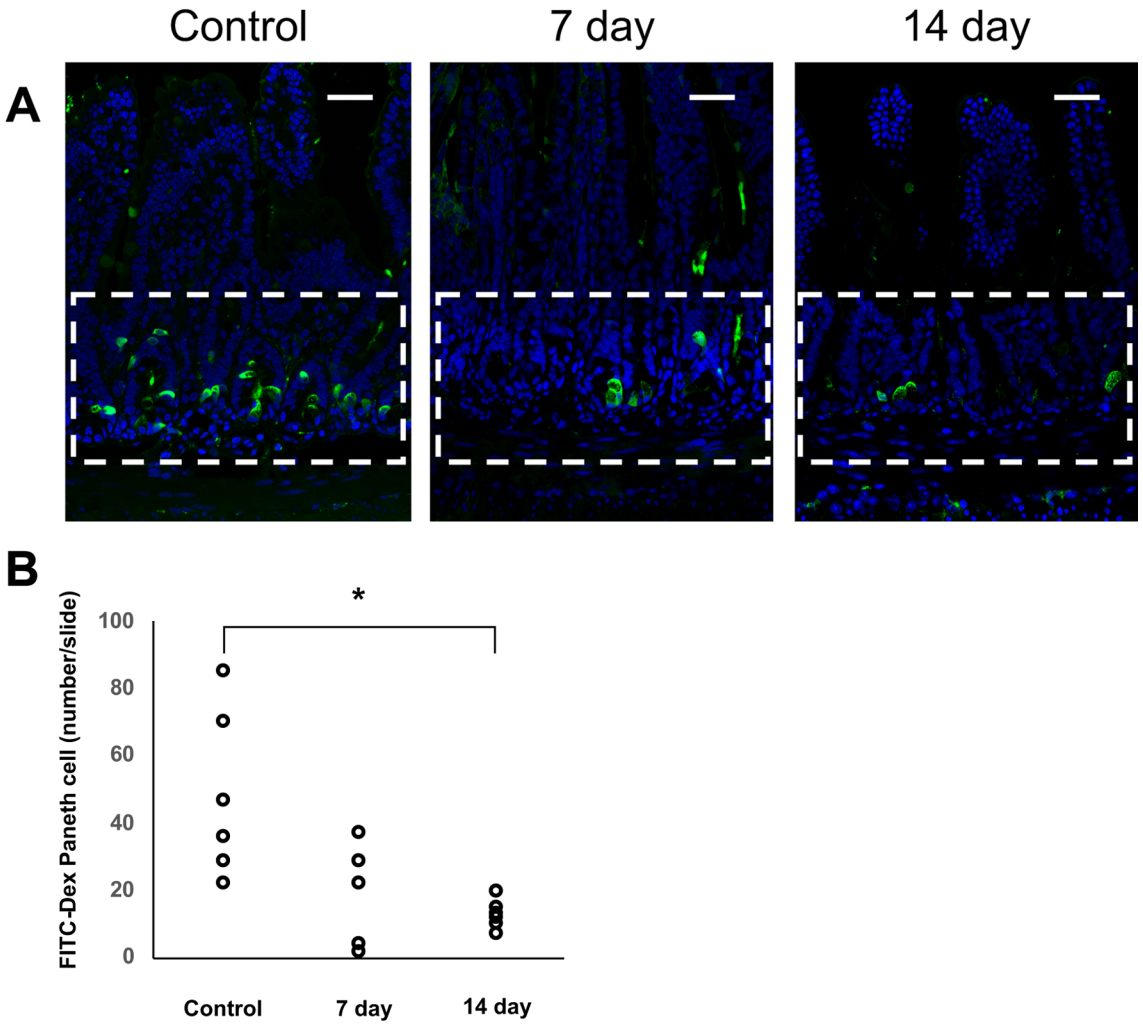


**Fig. 8.** Uptake of FITC-dextran in control and DSS mice on days 7 and 14. **A**) Fluorescence microscopic images of the ileum. The dashed square shows the crypt zone. Bars = 50 µm. **B**) Quantification of the FITC-dextran-positive Paneth cell number per slide. Statistically significant differences were set at a $p$-value < 0.05 (*).

crypts contained FITC in the cytoplasm (Fig. 6B).

To investigate whether the FITC-dextran uptake was due to dextran, we administered FITC alone and in combination with dextran, and compared it with the administration of FITC-dextran. When FITC was administered alone, there were almost no FITC-positive cells in the crypt; however, when FITC and dextran were administered concurrently, there were some FITC-positive cells, although not as many as with FITC-dextran (Fig. 7). We performed morphometric analysis of the effect of DSS on FITC-dextran uptake by Paneth cells. Compared to the control, the number of FITC-dextran positive Paneth cells decreased on day 7 and was significantly lower on day 14 ($p < 0.05$; Fig. 8).

## IV. Discussion

This experiment was designed with an inflammatory phase on the seventh day, and a recovery phase on the fourteenth day after DSS administration [41]. On day 7, severe damages occurred in the distal colon. However, in the ileum, enlarged crypts and hypertrophic Paneth cells were observed despite no significant changes in the number of Paneth cells. The amount of Muc2-positive mucus in goblet cells and their secretion into the lumen increased. Therefore, we postulate that the expansion of the crypt is caused by a change in Paneth cell morphology with excessive secretory granule production and that the activity of goblet cells is temporarily increased to protect the epithelium during inflammation.

*In situ* hybridization with *Atoh1* and immunohistochemistry for lysozyme revealed that the number of *Atoh1*-positive cells was reduced on day 7 but increased and dispersed in villi and crypts on day 14. Atoh1, a secretory cell differentiation factor, is expressed at higher levels in secretory progenitor and mature goblet cells [20, 39]. During the inflammatory phase, the differentiation into secretory cells was inhibited. However, during recovery, differentiation and maturation of secretory cells appeared to

occur in a different manner compared to normal epithelium turnover. *In situ* hybridization with *Lgr5* and immunohistochemistry for OLFM4, both stem cell markers, decreased during the inflammation phase. These findings are consistent with a previous report of DSS colitis in LGR5-EGFP mice [35]. In our study, *Lgr5*-positive cells were observed at the +4 cell position above Paneth cells on day 7. These cells were thought to become a supply source of ISCs [5]. This mechanism might be responsible for the recovery of *Lgr5*-positive cells on day 14. It has been reported that Paneth cell also dedifferentiate into Lgr5+ stem cells [35]. However, we did not observe a marked decrease in the number of Paneth cells in this study. Therefore, the possibility of Paneth cell dedifferentiation was considered minimal. Localization of *Lgr5*- and OLFM4-positive cells did not match exactly on day 7. OLFM4 displays mucin-like features and has been found to protects against mucosal damage [11]. These inconsistencies in localization indicated that the possibility of an active release and/or low expression level of OLFM4 protein during inflammation results in cellular OLFM4 decrease. TNF-α-treated organoids from IBD patient colons increased OLFM4 expression, and OLFM4-positive cells did not only occur in crypts but also in villi during the inflammatory phase [19]. However, no OLFM4-positive cells were found in villi during inflammation in our experiment, indicating that this was due to a difference in pathophysiology.

On day 7, lectin histochemistry revealed that the WGA- and UEA 1-positive mucus granules of goblet cells were enlarged and aggressively released into the lumen, indicating goblet cell hyperactivity. Nucleotide-binding oligomerization domain, leucine-rich Repeat and Pyrin domain-containing (NLRP) 6 deletion was reported to impair mucus secretion and lead to goblet cell hyperplasia [42]. Our results suggest that these alterations are caused by goblet cell hyperfunction, rather than hyperplasia derived from the decreased secretion. In Paneth cells, secretory granules were positive for WGA and UEA 1 in the control and DSS groups on day 14, while UEA 1 reactivity decreased on day 7. The secretory granules of Paneth cells are modified with α-1,2-fucose and are known to be important in the regulation of bacterial symbiosis [16]. The decrease in α-1,2 fucose modification during the inflammation phase may interfere with interactions with the bacterial flora.

In the DSS colitis model, the small intestine was not considered seriously affected. According to our findings, mucus hypersecretion occurs during the inflammatory phase, followed by an increase in differentiation into secretory cells during the recovery phase. These reactions result in preservation of the epithelium and may be related to the slight change in histological morphology.

FITC-dextran and HRP (data not shown) were administered into the ileum to examine epithelial barrier function. The epithelium appeared to be intact, and cellular junctions were not affected by DSS treatment. Unexpectedly, macromolecular uptake was observed. Macromolecules are rarely taken up by mature epithelial cells except by M cells under normal conditions. A recent study reported that goblet cells incorporate 10 kDa dextran [13]. In our study, OLFM4 positive-ISCs, lysozyme and Muc2 double positive-Paneth cells, and Muc2 positive-goblet cells in the ileum could take up 40 kDa FITC-dextran from the lumen, while HRP, with the same molecular weight (40 kDa), was not taken up (data not shown). In Paneth cells, FITC-dextran uptake may occur by direct membrane permeabilization, endocytosis, transporter-associated mechanisms, or a combination of these. We observed few colocalizations of FITC conjugate dextran and endosome markers by immunohistochemistry, indicating that a small portion of macromolecule uptake might have occurred by endocytosis (data not shown).

The number of macromolecules taken up by Paneth cells was lower in the inflammatory and recovery phases compared to the control. On day 14, the morphology of Paneth cells appeared to be restored to normal conditions, but their function did not seem to be fully recovered in the ileum. These results indicate that the functional maturation level of Paneth cells differed between the recovery phase and control. A previous study suggested that Paneth cell dysfunction causes CD and highlighted the significance of investigating the association between Paneth cell function and IBD pathogenesis [7]. Goblet cells have been reported to function not only in the innate immune system but also as regulators of acquired immunity that capture pathogens and transmit information to dendritic cells [21, 22]. Goblet cells and Paneth cells are closely related cells, and they have the same cell lineage of differentiation [12, 25]. As with goblet cells, Paneth cells may contribute to the immune function through macromolecule uptake. A delay in the recovery of the macromolecular uptake function may be associated with prolonged intestinal inflammation. However, the present approach was insufficient to uncover these possibilities. This study has two limitations: 1) the significance of Paneth cell uptake is unclear, and 2) it was impossible to distinguish whether the phenomena in secretory cells were direct results of DSS or due to indirect effects from colon inflammation. Further studies on Paneth cell absorption using electron microscopy and intestinal organoids are required to clarify these points. Although DSS is thought to induce inflammation in the large intestine without affecting the small intestine, alterations have been observed in secretory functions, including cellular morphology. Attenuation of the fucosylation of secretory granules and reduction in macromolecular uptake may affect the gut microbiota and immunological function, giving rise to the onset, exacerbation, and spread of intestinal inflammation.

To understand the pathogenesis of IBD, further research is needed to investigate how alterations in the secretory cells of the small intestine, including Paneth cells, affect the gut.

## V. Competing Interests

The authors have no relevant financial or non-financial interests to disclose.

## VI. Authors' Contributions

All the authors contributed to the conception and design of this study. Material preparation, data collection, and analyses were performed by Kenta Nakamura and Ryoko Baba. Statistical analyses were performed by Keiji Kokubu. Kenta Nakamura wrote the first draft of this manuscript. Hiroyuki Morimoto performed editing. All authors commented on the previous versions of the manuscript. All authors have read and approved the final manuscript.

## VII. Data Availability

All data generated or analyzed in this study are included in the published article.

## VIII. Acknowledgments

This work was supported by JSPS KAKENHI (grant numbers 21K07927 [HM] and 21K08017 [RB)].

## IX. References

1. Asfaha, S., Hayakawa, Y., Muley, A., Stokes, S., Graham, T. A., Ericksen, R. E., *et al.* (2015) *Krt19*$^{+}$*/Lgr5*$^{-}$ Cells Are Radioresistant Cancer-Initiating Stem Cells in the Colon and Intestine. *Cell Stem Cell* 16; 627–638.
2. Baba, R., Kokubu, K., Nakamura, K., Fujita, M. and Morimoto, H. (2022) Paneth cell maturation is related to epigenetic modification during neonatal-weaning transition. *Histochem. Cell Biol.* 158; 5–13.
3. Barker, N., van de Wetering, M. and Clevers, H. (2008) The intestinal stem cell. *Genes Dev.* 22; 1856–1864.
4. Barker, N. and Clevers, H. (2010) Leucine-rich repeat-containing G-protein-coupled receptors as markers of adult stem cells. *Gastroenterology* 138; 1681–1696.
5. Barker, N. (2014) Adult intestinal stem cells: critical drivers of epithelial homeostasis and regeneration. *Nat. Rev. Mol. Cell Biol.* 15; 19–33.
6. Barriga, F. M., Montagni, E., Mana, M., Mendez-Lago, M., Hernando-Momblona, X., Sevillano, M., *et al.* (2017) Mex3a Marks a Slowly Dividing Subpopulation of Lgr5+ Intestinal Stem Cells. *Cell Stem Cell* 20; 801–816.e7.
7. Bevins, C. L. and Salzman, N. H. (2011) Paneth cells, antimicrobial peptides and maintenance of intestinal homeostasis. *Nat. Rev. Microbiol.* 9; 356–368.
8. Chassaing, B., Aitken, J. D., Malleshappa, M. and Vijay-Kumar, M. (2014) Dextran sulfate sodium (DSS)-induced colitis in mice. *Curr. Protoc. Immunol.* 104; 15.25.1–15.25.14.
9. Eriguchi, Y., Takashima, S., Oka, H., Shimoji, S., Nakamura, K., Uryu, H., *et al.* (2012) Graft-versus-host disease disrupts intestinal microbial ecology by inhibiting Paneth cell production of alpha-defensins. *Blood* 120; 223–231.
10. Gersemann, M., Becker, S., Kubler, I., Koslowski, M., Wang, G., Herrlinger, K. R., *et al.* (2009) Differences in goblet cell differentiation between Crohn's disease and ulcerative colitis. *Differentiation* 77; 84–94.
11. Gersemann, M., Becker, S., Nuding, S., Antoni, L., Ott, G., Fritz, P., *et al.* (2012) Olfactomedin-4 is a glycoprotein secreted into mucus in active IBD. *J. Crohns Colitis* 6; 425–434.
12. Gregorieff, A., Stange, D. E., Kujala, P., Begthel, H., van den Born, M., Korving, J., *et al.* (2009) The ets-domain transcription factor Spdef promotes maturation of goblet and paneth cells in the intestinal epithelium. *Gastroenterology* 137; 1333–1345.e1-3.
13. Gustafsson, J. K., Davis, J. E., Rappai, T., McDonald, K. G., Kulkarni, D. H., Knoop, K. A., *et al.* (2021) Intestinal goblet cells sample and deliver lumenal antigens by regulated endocytic uptake and transcytosis. *Elife* 10; e67292.
14. Habermann, F. A., Kaltner, H., Higuero, A. M., Garcia Caballero, G., Ludwig, A. K., C Manning, J., *et al.* (2021) What Cyto- and Histochemistry Can Do to Crack the Sugar Code. *Acta Histochem. Cytochem.* 54; 31–48.
15. Hamilton, M. J., Makrauer, F. M., Golden, K., Wang, H., Friedman, S., Burakoff, R. B., *et al.* (2016) Prospective Evaluation of Terminal Ileitis in a Surveillance Population of Patients with Ulcerative Colitis. *Inflamm. Bowel Dis.* 22; 2448–2455.
16. Hashiguchi, H., Tsukamoto, Y., Ogawa, M., Tashima, Y., Takeuchi, H., Nakamura, M., *et al.* (2020) Glycoproteomic analysis identifies cryptdin-related sequence 1 as *O*-glycosylated protein modified with α1,2-fucose in the small intestine. *Arch. Biochem. Biophys.* 695; 108653.
17. Higo, S., Ishii, H. and Ozawa, H. (2023) Recent Advances in High-sensitivity *In Situ* Hybridization and Costs and Benefits to Consider When Employing These Methods. *Acta Histochem. Cytochem.* 56; 49–54.
18. Kelly, P., Feakins, R., Domizio, P., Murphy, J., Bevins, C., Wilson, J., *et al.* (2004) Paneth cell granule depletion in the human small intestine under infective and nutritional stress. *Clin. Exp. Immunol.* 135; 303–309.
19. Kuno, R., Ito, G., Kawamoto, A., Hiraguri, Y., Sugihara, H. Y., Takeoka, S., *et al.* (2021) Notch and TNF-α signaling promote cytoplasmic accumulation of OLFM4 in intestinal epithelium cells and exhibit a cell protective role in the inflamed mucosa of IBD patients. *Biochem. Biophys. Rep.* 25; 100906.
20. Lo, Y. H., Chung, E., Li, Z., Wan, Y. W., Mahe, M. M., Chen, M. S., *et al.* (2017) Transcriptional Regulation by ATOH1 and its Target SPDEF in the Intestine. *Cell Mol Gastroenterol. Hepatol.* 3; 51–71.
21. Ma, J., Rubin, B. K. and Voynow, J. A. (2018) Mucins, Mucus, and Goblet Cells. *Chest* 154; 169–176.
22. McDole, J. R., Wheeler, L. W., McDonald, K. G., Wang, B., Konjufca, V., Knoop, K. A., *et al.* (2012) Goblet cells deliver luminal antigen to CD103$^{+}$ dendritic cells in the small intestine. *Nature* 483; 345–349.
23. Miller, A., Cutroneo, G., Lombardo, G. P., D'Angelo, R., Pallio, S., Migliorato, A., *et al.* (2023) Association between neuropeptides and mucins in Crohn's disease mucous cells. *Acta Histochem.* 125; 152115.
24. Montgomery, R. K., Carlone, D. L., Richmond, C. A., Farilla, L., Kranendonk, M. E., Henderson, D. E., *et al.* (2011) Mouse telomerase reverse transcriptase (mTert) expression marks slowly cycling intestinal stem cells. *Proc. Natl. Acad. Sci. U S A* 108; 179–184.
25. Noah, T. K., Kazanjian, A., Whitsett, J. and Shroyer, N. F. (2010) SAM pointed domain ETS factor (SPDEF) regulates terminal differentiation and maturation of intestinal goblet cells. *Exp. Cell. Res.* 316; 452–465.
26. Nowarski, R., Jackson, R., Gagliani, N., de Zoete, M. R., Palm,

N. W., Bailis, W., *et al.* (2015) Epithelial IL-18 Equilibrium Controls Barrier Function in Colitis. *Cell.* 163; 1444–1456.
27. Pelaseyed, T., Bergström, J. H., Gustafsson, J. K., Ermund, A., Birchenough, G. M., Schütte, A., *et al.* (2014) The mucus and mucins of the goblet cells and enterocytes provide the first defense line of the gastrointestinal tract and interact with the immune system. *Immunol. Rev.* 260; 8–20.
28. Potten, C. S., Hume, W. J., Reid, P. and Cairns, J. (1978) The segregation of DNA in epithelial stem cells. *Cell.* 15; 899–906.
29. Potten, C. S., Owen, G. and Booth, D. (2002) Intestinal stem cells protect their genome by selective segregation of template DNA strands. *J. Cell Sci.* 115; 2381–2388.
30. Raouf, Z., Steinway, S. N., Scheese, D., Lopez, C. M., Duess, J. W., Tsuboi, K., *et al.* (2024) Colitis-Induced Small Intestinal Hypomotility Is Dependent on Enteroendocrine Cell Loss in Mice. *Cell. Mol. Gastroenterol. Hepatol.* 18; 53–70.
31. Ritchie, J. M., Rui, H., Bronson, R. T. and Waldor, M. K. (2010) Back to the future: studying cholera pathogenesis using infant rabbits. *mBio* 1; e00047–10.
32. Ritchie, J. M., Rui, H., Zhou, X., Iida, T., Kodoma, T., Ito, S., *et al.* (2012) Inflammation and disintegration of intestinal villi in an experimental model for *Vibrio parahaemolyticus*-induced diarrhea. *PLoS Pathog.* 8; e1002593.
33. Robbe Masselot, C., Cordier, C., Marsac, B., Nachury, M., Leonard, R. and Sendid, B. (2023) Human Fecal Mucin Glycosylation as a New Biomarker in Inflammatory Bowel Diseases. *Inflamm. Bowel Dis.* 29; 167–171.
34. Sato, T., van Es, J. H., Snippert, H. J., Stange, D. E., Vries, R. G., van den Born, M., *et al.* (2011) Paneth cells constitute the niche for Lgr5 stem cells in intestinal crypts. *Nature* 469; 415–418.
35. Schmitt, M., Schewe, M., Sacchetti, A., Feijtel, D., van de Geer, W. S., Teeuwssen, M., *et al.* (2018) Paneth Cells Respond to Inflammation and Contribute to Tissue Regeneration by Acquiring Stem-like Features through SCF/c-Kit Signaling. *Cell Rep.* 24; 2312–2328.e2317.
36. Singh, R., Balasubramanian, I., Zhang, L. and Gao, N. (2020) Metaplastic Paneth Cells in Extra-Intestinal Mucosal Niche Indicate a Link to Microbiome and Inflammation. *Front. Physiol.* 11; 280.
37. Tanaka, M., Saito, H., Kusumi, T., Fukuda, S., Shimoyama, T., Sasaki, Y., *et al.* (2001) Spatial distribution and histogenesis of colorectal Paneth cell metaplasia in idiopathic inflammatory bowel disease. *J. Gastroenterol. Hepatol.* 16; 1353–1359.
38. Toth, Z. E. and Mezey, E. (2007) Simultaneous visualization of multiple antigens with tyramide signal amplification using antibodies from the same species. *J. Histochem. Cytochem.* 55; 545–554.
39. Verhagen, M. P., Joosten, R., Schmitt, M., Valimaki, N., Sacchetti, A., Rajamaki, K., *et al.* (2024) Non-stem cell lineages as an alternative origin of intestinal tumorigenesis in the context of inflammation. *Nat. Genet.* 56; 1456–1467.
40. Wang, Z. and Shen, J. (2024) The role of goblet cells in Crohn's disease. *Cell Biosci.* 14; 43.
41. Wirtz, S., Popp, V., Kindermann, M., Gerlach, K., Weigmann, B., Fichtner-Feigl, S., *et al.* (2017) Chemically induced mouse models of acute and chronic intestinal inflammation. *Nat. Protoc.* 12; 1295–1309.
42. Wlodarska, M., Thaiss, C. A., Nowarski, R., Henao-Mejia, J., Zhang, J. P., Brown, E. M., *et al.* (2014) NLRP6 inflammasome orchestrates the colonic host-microbial interface by regulating goblet cell mucus secretion. *Cell* 156; 1045–1059.
43. Yamamoto, T., Maruyama, Y., Umegae, S., Matsumoto, K. and Saniabadi, A. R. (2008) Mucosal inflammation in the terminal ileum of ulcerative colitis patients: endoscopic findings and cytokine profiles. *Dig. Liver Dis.* 40; 253–259.
44. Yang, E. and Shen, J. (2021) The roles and functions of Paneth cells in Crohn's disease: A critical review. *Cell Prolif.* 54; e12958.
45. Yang, S. and Yu, M. (2021) Role of Goblet Cells in Intestinal Barrier and Mucosal Immunity. *J. Inflamm. Res.* 14; 3171–3183.
46. Zheng, X., Tsuchiya, K., Okamoto, R., Iwasaki, M., Kano, Y., Sakamoto, N., *et al.* (2011) Suppression of hath1 gene expression directly regulated by hes1 via notch signaling is associated with goblet cell depletion in ulcerative colitis. *Inflamm. Bowel Dis.* 17; 2251–2260.